Study of $B^0 \to \rho^{\pm}\pi^{\mp}$ Time-Dependent CP Violation at Belle

C. C. Wang,[25] K. Abe,[7] K. Abe,[40] T. Abe,[7] I. Adachi,[7] H. Aihara,[42] Y. Asano,[46] T. Aushev,[11] A. M. Bakich,[37] Y. Ban,[32] A. Bay,[16] I. Bedny,[1] U. Bitenc,[12] I. Bizjak,[12] S. Blyth,[25] A. Bondar,[1] A. Bozek,[26] M. Bračko,[18,12] T. E. Browder,[6] P. Chang,[25] Y. Chao,[25] K.-F. Chen,[25] W. T. Chen,[22] B. G. Cheon,[2] S.-K. Choi,[5] Y. Choi,[36] A. Chuvikov,[33] S. Cole,[37] M. Dash,[47] L. Y. Dong,[9] J. Dragic,[19] A. Drutskoy,[3] S. Eidelman,[1] V. Eiges,[11] T. Gershon,[7] G. Gokhroo,[38] R. Guo,[23] J. Haba,[7] N. C. Hastings,[7] K. Hayasaka,[20] H. Hayashii,[21] M. Hazumi,[7] T. Hokuue,[20] Y. Hoshi,[40] S. Hou,[22] W.-S. Hou,[25] Y. B. Hsiung,[25,*] T. Iijima,[20] A. Imoto,[21] K. Inami,[20] A. Ishikawa,[7] H. Ishino,[43] K. Itoh,[42] R. Itoh,[7] H. Iwasaki,[7] Y. Iwasaki,[7] H. Kakuno,[42] J. H. Kang,[48] J. S. Kang,[14] P. Kapusta,[26] N. Katayama,[7] T. Kawasaki,[28] H. R. Khan,[43] H. Kichimi,[7] H. J. Kim,[15] K. Kinoshita,[3] P. Križan,[17,12] P. Krokovny,[1] S. Kumar,[31] Y.-J. Kwon,[48] J. S. Lange,[4] S. E. Lee,[35] Y.-J. Lee,[25] T. Lesiak,[26] J. Li,[34] A. Limosani,[19] S.-W. Lin,[25] J. MacNaughton,[10] T. Matsumoto,[44] A. Matyja,[26] Y. Mikami,[41] W. Mitaroff,[10] H. Miyata,[28] R. Mizuk,[11] D. Mohapatra,[47] T. Mori,[43] Y. Nagasaka,[8] T. Nakadaira,[42] E. Nakano,[29] M. Nakao,[7] Z. Natkaniec,[26] S. Nishida,[7] O. Nitoh,[45] T. Nozaki,[7] S. Ogawa,[39] T. Ohshima,[20] T. Okabe,[20] S. Okuno,[13] S. L. Olsen,[6] W. Ostrowicz,[26] H. Ozaki,[7] P. Pakhlov,[11] C. W. Park,[36] N. Parslow,[37] L. S. Peak,[37] L. E. Piilonen,[47] F. J. Ronga,[7] M. Rozanska,[26] H. Sagawa,[7] S. Saitoh,[7] Y. Sakai,[7] N. Sato,[20] T. Schietinger,[16] O. Schneider,[16] J. Schümann,[25] A. J. Schwartz,[3] S. Semenov,[11] K. Senyo,[20] M. E. Sevior,[19] H. Shibuya,[39] J. B. Singh,[31] A. Somov,[3] R. Stamen,[7] S. Stanič,[46,†] M. Starič,[12] K. Sumisawa,[30] T. Sumiyoshi,[44] S. Y. Suzuki,[7] O. Tajima,[41] F. Takasaki,[7] K. Tamai,[7] M. Tanaka,[7] G. N. Taylor,[19] Y. Teramoto,[29] X. C. Tian,[32] K. Trabelsi,[6] T. Tsukamoto,[7] S. Uehara,[7] T. Uglov,[11] K. Ueno,[25] S. Uno,[7] G. Varner,[6] K. E. Varvell,[37] S. Villa,[16] C. H. Wang,[24] M.-Z. Wang,[25] M. Watanabe,[28] B. D. Yabsley,[47] Y. Yamada,[7] A. Yamaguchi,[41] Y. Yamashita,[27] M. Yamauchi,[7] J. Ying,[32] Y. Yusa,[41] J. Zhang,[7] L. M. Zhang,[34] Z. P. Zhang,[34] V. Zhilich,[1] T. Ziegler,[33] and D. Žontar[17,12]

(Belle Collaboration)

[1]*Budker Institute of Nuclear Physics, Novosibirsk*
[2]*Chonnam National University, Kwangju*
[3]*University of Cincinnati, Cincinnati, Ohio 45221*
[4]*University of Frankfurt, Frankfurt*
[5]*Gyeongsang National University, Chinju*
[6]*University of Hawaii, Honolulu, Hawaii 96822*
[7]*High Energy Accelerator Research Organization (KEK), Tsukuba*
[8]*Hiroshima Institute of Technology, Hiroshima*
[9]*Institute of High Energy Physics, Chinese Academy of Sciences, Beijing*
[10]*Institute of High Energy Physics, Vienna*
[11]*Institute for Theoretical and Experimental Physics, Moscow*
[12]*J. Stefan Institute, Ljubljana*
[13]*Kanagawa University, Yokohama*
[14]*Korea University, Seoul*
[15]*Kyungpook National University, Taegu*
[16]*Swiss Federal Institute of Technology of Lausanne, EPFL, Lausanne*
[17]*University of Ljubljana, Ljubljana*
[18]*University of Maribor, Maribor*
[19]*University of Melbourne, Victoria*
[20]*Nagoya University, Nagoya*
[21]*Nara Women's University, Nara*
[22]*National Central University, Chung-li*
[23]*National Kaohsiung Normal University, Kaohsiung*
[24]*National United University, Miao Li*
[25]*Department of Physics, National Taiwan University, Taipei*
[26]*H. Niewodniczanski Institute of Nuclear Physics, Krakow*
[27]*Nihon Dental College, Niigata*
[28]*Niigata University, Niigata*
[29]*Osaka City University, Osaka*
[30]*Osaka University, Osaka*
[31]*Panjab University, Chandigarh*

[32]Peking University, Beijing
[33]Princeton University, Princeton, New Jersey 08545
[34]University of Science and Technology of China, Hefei
[35]Seoul National University, Seoul
[36]Sungkyunkwan University, Suwon
[37]University of Sydney, Sydney, New South Wales
[38]Tata Institute of Fundamental Research, Bombay
[39]Toho University, Funabashi
[40]Tohoku Gakuin University, Tagajo
[41]Tohoku University, Sendai
[42]Department of Physics, University of Tokyo, Tokyo
[43]Tokyo Institute of Technology, Tokyo
[44]Tokyo Metropolitan University, Tokyo
[45]Tokyo University of Agriculture and Technology, Tokyo
[46]University of Tsukuba, Tsukuba
[47]Virginia Polytechnic Institute and State University, Blacksburg, Virginia 24061
[48]Yonsei University, Seoul

(Received 1 August 2004; published 1 April 2005)

We present a time-dependent analysis of CP violation in $B^0 \to \rho^\pm \pi^\mp$ decays based on a 140 fb^{-1} data sample collected at the $\Upsilon(4S)$ resonance with the Belle detector at KEKB. We obtain the charge asymmetry $\mathcal{A}_{CP}^{\rho\pi} = -0.16 \pm 0.10(\text{stat}) \pm 0.02(\text{syst})$. An unbinned maximum-likelihood fit to the Δt distributions yields $C_{\rho\pi} = 0.25 \pm 0.17(\text{stat})^{+0.02}_{-0.06}(\text{syst})$, $\Delta C_{\rho\pi} = 0.38 \pm 0.18(\text{stat})^{+0.02}_{-0.04}(\text{syst})$, $S_{\rho\pi} = -0.28 \pm 0.23(\text{stat})^{+0.10}_{-0.08}(\text{syst})$, and $\Delta S_{\rho\pi} = -0.30 \pm 0.24(\text{stat}) \pm 0.09(\text{syst})$. The direct CP violation parameters for $B \to \rho^+\pi^-$ and $B \to \rho^-\pi^+$ decays are $\mathcal{A}_{\rho\pi}^{+-} = -0.02 \pm 0.16(\text{stat})^{+0.05}_{-0.02}(\text{syst})$ and $\mathcal{A}_{\rho\pi}^{-+} = -0.53 \pm 0.29(\text{stat})^{+0.09}_{-0.04}(\text{syst})$.

DOI: 10.1103/PhysRevLett.94.121801 PACS numbers: 13.25.Hw, 11.30.Er, 12.15.Hh, 14.40.Nd

In the standard model of elementary particles, CP violation arises from the Kobayashi-Maskawa phase [1] in the quark-mixing matrix. CP violating effects in the B meson system can be parametrized in terms of three angles, ϕ_1, ϕ_2, and ϕ_3 (also written β, α, and γ, respectively). Recently, the CP violation parameter ϕ_2 was studied by the Belle [2] and *BABAR* [3] collaborations using $B \to \pi^+\pi^-$ decays that proceed by $b \to u\bar{u}d$ transitions. Here we present a study of $B \to \rho^\pm\pi^\mp$ time-dependent CP asymmetry, which offers another way to constrain ϕ_2. Both direct and indirect CP violation can be probed in this decay. Since $B \to \rho^\pm\pi^\mp$ is not a CP eigenstate decay, four decay modes with different charge and flavor combinations in the neutral B meson system must be considered.

In the decay chain $\Upsilon(4S) \to B^0\overline{B}^0 \to (\rho^\pm\pi^\mp) f_{\text{tag}}$, one of the B mesons decays at time $t_{\rho\pi}$ to $\rho^\pm\pi^\mp$ and the other meson decays at time t_{tag} to a final state f_{tag} that distinguishes between B^0 and $\overline{B}^0$. The decay rate for $B^0(\overline{B}^0) \to \rho^\pm\pi^\mp$ has a time dependence given by [4]

$$\mathcal{P}_q^{\rho^\pm\pi^\mp}(\Delta t) = (1 \pm \mathcal{A}_{CP}^{\rho\pi}) \frac{e^{-|\Delta t|/\tau_{B^0}}}{8\tau_{B^0}} \times \{1 + q[(S_{\rho\pi} \pm \Delta S_{\rho\pi}) \sin(\Delta m_d \Delta t) - (C_{\rho\pi} \pm \Delta C_{\rho\pi}) \cos(\Delta m_d \Delta t)]\}, \quad (1)$$

where τ_{B^0} is the B^0 lifetime, Δm_d is the mass difference between the two B^0 mass eigenstates, $\Delta t = t_{\rho\pi} - t_{\text{tag}}$, and the b-flavor charge $q = +1(-1)$ when the tagging B meson is a $B^0(\overline{B}^0)$. The time and flavor integrated charge asymmetry $\mathcal{A}_{CP}^{\rho\pi}$ is defined as

$$\mathcal{A}_{CP}^{\rho\pi} = \frac{N(\rho^+\pi^-) - N(\rho^-\pi^+)}{N(\rho^+\pi^-) + N(\rho^-\pi^+)}, \quad (2)$$

where $N(\rho^+\pi^-)$ and $N(\rho^-\pi^+)$ are the sum of the yields for B^0 and $\overline{B}^0$ decays to $\rho^+\pi^-$ and $\rho^-\pi^+$, respectively. The mixing-induced CP violation parameter $S_{\rho\pi}$ is related to ϕ_2, and $C_{\rho\pi}$ is the flavor-dependent direct CP violation parameter. The asymmetry between the decay rates, $\Gamma(B^0 \to \rho^+\pi^-) + \Gamma(\overline{B}^0 \to \rho^-\pi^+)$ and $\Gamma(B^0 \to \rho^-\pi^+) + \Gamma(\overline{B}^0 \to \rho^+\pi^-)$, is described by $\Delta C_{\rho\pi}$, while the strong phase difference between the amplitudes contributing to $B^0 \to \rho\pi$ decays is described by $\Delta S_{\rho\pi}$. These parameters are related to ϕ_2 as $S_{\rho\pi} \pm \Delta S_{\rho\pi} = \sqrt{1 - (C_{\rho\pi} \pm \Delta C_{\rho\pi})^2} \times \sin(2\phi_{2\text{eff}}^\pm \pm \delta)$, where $2\phi_{2\text{eff}}^\pm = \arg[(q/p)(\bar{A}_{\rho\pi}^\pm / A_{\rho\pi}^\mp)]$ and $\delta = \arg[A_{\rho\pi}^- / A_{\rho\pi}^+]$; $\arg[q/p]$ is the B^0-$\overline{B}^0$ mixing phase. The terms $A_{\rho\pi}^+(\bar{A}_{\rho\pi}^+)$ and $A_{\rho\pi}^-(\bar{A}_{\rho\pi}^-)$ denote the transition amplitudes for the processes $B^0(\overline{B}^0) \to \rho^+\pi^-$ and $B^0(\overline{B}^0) \to \rho^-\pi^+$, respectively. The angles $\phi_{2\text{eff}}^\pm$ are equal to ϕ_2 if there is no penguin contribution. The effect of direct CP violation can also be expressed in terms of another set of parameters, $\mathcal{A}_{\rho\pi}^{+-}$ and $\mathcal{A}_{\rho\pi}^{-+}$:

$$\mathcal{A}_{\rho\pi}^{\pm\mp} = \frac{N(\overline{B}^0 \to \rho^\mp\pi^\pm) - N(B^0 \to \rho^\pm\pi^\mp)}{N(\overline{B}^0 \to \rho^\mp\pi^\pm) + N(B^0 \to \rho^\pm\pi^\mp)} = \mp \frac{\mathcal{A}_{CP}^{\rho\pi} \pm C_{\rho\pi} \pm \mathcal{A}_{CP}^{\rho\pi} \cdot \Delta C_{\rho\pi}}{1 \pm \Delta C_{\rho\pi} \pm \mathcal{A}_{CP}^{\rho\pi} \cdot C_{\rho\pi}}, \quad (3)$$

The strategy of this analysis is to reconstruct final states in quasi-two-body decays $B^0 \to (\pi^\pm\pi^0)\pi^\mp$, which correspond to distinct bands in the $\pi^+\pi^-\pi^0$ Dalitz plot. We exclude the interference region where the ρ charge is ambiguous, and neglect possible residual interference effects.

The results for this analysis are based on 140 fb^{-1} of integrated luminosity, which corresponds to 152×10^6 produced $B\overline{B}$ pairs. The data were collected with the Belle detector at the KEKB asymmetric-energy e^+e^- collider [5], which collides 8.0 GeV e^- and 3.5 GeV e^+ beams. The $\Upsilon(4S)$ is produced with a Lorentz boost of $\beta\gamma = 0.425$ nearly along the electron beam line. Since the B^0 and $\overline{B}^0$ mesons are approximately at rest in the $\Upsilon(4S)$ center-of-mass (c.m.) system, Δt can be determined from Δz, the displacement in z between the $\rho^\pm\pi^\mp$ and $f_{\rm tag}$ decay vertices: $\Delta t \simeq (z_{\rho^\pm\pi^\mp} - z_{\rm tag})/\beta\gamma c$. The z axis is antiparallel to the positron beam.

The Belle detector [6] is a large-solid-angle general purpose spectrometer that consists of a silicon vertex detector (SVD), a central drift chamber (CDC), an array of aerogel threshold Čerenkov counters (ACC), time-of-flight (TOF) scintillation counters, and an electromagnetic calorimeter (ECL) comprised of CsI(Tl) crystals located inside a superconducting solenoid coil that provides a 1.5 T magnetic field. An iron flux return located outside of the coil is instrumented to detect K_L^0 mesons and identify muons.

To reconstruct $B^0 \to \rho^\pm\pi^\mp$ candidates, we combine pairs of oppositely charged tracks with π^0 candidates. Each charged track is required to have transverse momenta greater than 100 MeV/c in the laboratory frame with SVD hits. Charged tracks are identified as pions by combining information from the ACC, CDC, and TOF. Electronlike tracks are rejected. The γ energies for π^0 candidates are required to be greater than 50 MeV if the photon is detected in the barrel ECL ($32° < \theta < 129°$); otherwise, the energy is required to be larger than 100 MeV, where θ denotes the polar angle with respect to the z axis. The π^0 candidates are selected from $\gamma\gamma$ pairs with invariant masses in the range $0.118\ {\rm GeV}/c^2 < M_{\gamma\gamma} < 0.150\ {\rm GeV}/c^2$, and momentum larger than 200 MeV/c in the laboratory frame. In addition, we require $|\cos\theta^{\pi^0}_{\rm dec}| < 0.95$, where $\theta^{\pi^0}_{\rm dec}$ is defined as the angle between the photon flight direction and the boost direction from the laboratory system in the π^0 rest frame, and we require the χ^2 of the π^0 mass-constrained fit to be less than 50 (this requirement is 99% efficient).

B meson candidates are reconstructed using the beam-energy constrained mass $M_{\rm bc} \equiv \sqrt{E^2_{\rm beam} - P^2_B}$ and the energy difference $\Delta E \equiv E_B - E_{\rm beam}$. The variables E_B and P_B are the reconstructed energy and momentum of the B candidate in the c.m. frame, and $E_{\rm beam}$ is the c.m. beam energy. The selection region is defined as $M_{\rm bc} > 5.2\ {\rm GeV}/c^2$ and $-0.3\ {\rm GeV} < \Delta E < 0.2\ {\rm GeV}$, and the signal region as $M_{\rm bc} > 5.27\ {\rm GeV}/c^2$ and $-0.10\ {\rm GeV} < \Delta E < 0.08\ {\rm GeV}$. The $B \to \rho^\pm\pi^\mp$ candidates are formed from three-body $B \to \pi^+\pi^-\pi^0$ decays with a $\pi^\pm\pi^0$ invariant mass in the range $0.57\ {\rm GeV}/c^2 < M_{\pi^\pm\pi^0} < 0.97\ {\rm GeV}/c^2$ and ρ helicity $|\cos\theta^\rho_{\rm hel}| > 0.5$, where $\theta^\rho_{\rm hel}$ is defined as the angle between the charged pion direction and the B^0 direction in the ρ rest frame. To avoid the region where the $\rho^+\pi^-$ and $\rho^-\pi^+$ contributions interfere, we exclude candidates with both $M_{\pi^+\pi^0}$ and $M_{\pi^-\pi^0}$ smaller than $1.22\ {\rm GeV}/c^2$. Candidates with $M_{\pi^+\pi^-} < 0.97\ {\rm GeV}/c^2$ are removed to avoid the region where the $\rho^+\pi^-$ or $\rho^-\pi^+$ bands overlap with $\rho^0\pi^0$.

To suppress the dominant $e^+e^- \to q\bar{q}$ continuum background ($q = u, d, s, c$), we form the likelihood ratio $\mathcal{R} = \mathcal{L}_{\rm s}/(\mathcal{L}_{\rm s} + \mathcal{L}_{\rm bkg})$, where $\mathcal{L}_{\rm s}$ and $\mathcal{L}_{\rm bkg}$ are likelihood functions for signal and continuum events, respectively. We use a Fisher discriminant based on five modified Fox-Wolfram moments [7], and the c.m. flight direction of the B (θ_B) with respect to the z axis to form the likelihood function. The signal likelihood $\mathcal{L}_{\rm s}$ is determined from a GEANT-based Monte Carlo (MC) simulation, and $\mathcal{L}_{\rm bkg}$ is based on $M_{\rm bc}$ sideband data, $M_{\rm bc} < 5.26\ {\rm GeV}/c^2$. The continuum background is reduced by requiring $\mathcal{R}$ to be greater than 0.8. If there is more than one candidate in an event, we select the candidate with the smallest sum of the χ^2 for the $\pi^+\pi^-$ vertex fit and the π^0 mass-constrained fit.

The flavor of the accompanying B meson is identified from the decay products not associated with the reconstructed $B^0 \to \rho^\pm\pi^\mp$ decay. We use the same method as used for the Belle $\sin 2\phi_1$ measurement [8,9]. Two parameters q and r are used to describe the flavor tagging information. The parameter q is defined in Eq. (1), and the parameter r is a MC-determined quality factor that ranges

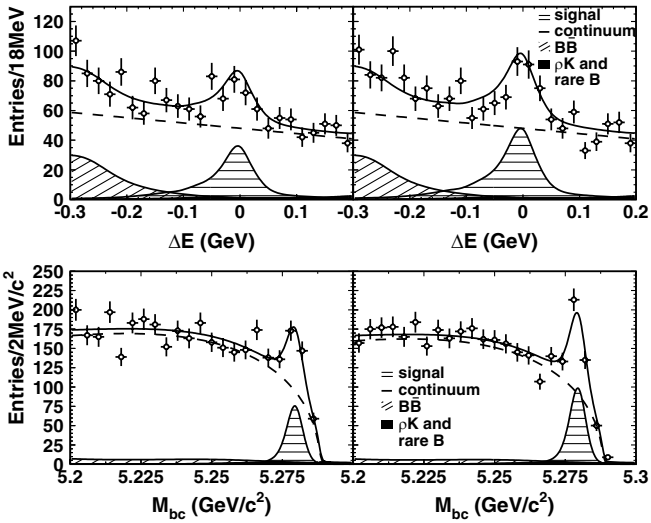

FIG. 1. ΔE (top) and $M_{\rm bc}$ (bottom) projections for the result of the 2D unbinned likelihood fit. The plots on the left are the results for the $\rho^+\pi^-$ candidates, while those on the right show the results for the $\rho^-\pi^+$ candidates.

from $r = 0$ for no flavor discrimination to $r = 1$ for unambiguous flavor assignment. It is used only to sort data into six r intervals. The vertex reconstruction algorithm is the same as that used for the $\sin 2\phi_1$ analysis [8].

Figure 1 shows the ΔE ($M_{\rm bc}$) distribution in the $M_{\rm bc}$ (ΔE) signal region for $B^0 \to \rho^\pm \pi^\mp$ candidates after flavor tagging and vertex reconstruction. The $\rho^\pm \pi^\mp$ signal yields are extracted from an unbinned maximum-likelihood fit to the two-dimensional ($M_{\rm bc}$, ΔE) distribution. The backgrounds are categorized as continuum $q\bar{q}$, $b \to c$ transitions ($B\overline{B}$), $B \to \rho K$, and rare charmless decays other than $B \to \rho K$ (rare B). The distributions for $\rho\pi$, $B\overline{B}$, ρK, and rare B events are obtained from MC simulations.

The $\rho\pi$ signal probability density function (PDF) contains two components: signal events reconstructed with the correct charge ($P_{\rho\pi}$) and those with incorrect charge ($P^{\rm wc}_{\rho\pi}$). The fraction of events with incorrect charge in the signal region due to combinations that include a random π^0 is estimated to be 2.7% from MC simulations and is fixed in the fit. The signal PDF shape is modeled by a smoothed histogram. The ΔE distributions for $B \to \rho\pi$ signal are parametrized separately for π^0 momentum below and above 1.2 GeV/c in the laboratory frame. The ΔE widths for $\rho\pi$ and ρK are calibrated from $D^{*0} \to D^0[K^-\pi^+]\pi^0$ data. The $B^+ \to D^0[K^-\pi^+\pi^0]\pi^+$ mode is used to calibrate the ΔE and $M_{\rm bc}$ peak positions. The $M_{\rm bc}$ and ΔE distributions for the continuum $q\bar{q}$ background are parametrized by an ARGUS function [10] and a linear function, respectively. The contributions from $B \to \rho K$ [with $\mathcal{B} = (9.0 \pm 1.6) \times 10^{-6}$ [11]] and from rare B decays are fixed in the fit, while the yields for $B \to \rho\pi$ signal, $B\overline{B}$ and continuum backgrounds, and the shape parameters for continuum are floated. From the selection region, we obtain 483 ± 46 $B \to \rho^\pm \pi^\mp$ events, and obtain a time and flavor integrated charge asymmetry $\mathcal{A}^{\rho\pi}_{CP} = -0.16 \pm 0.10$(stat).

The estimated yields for $B \to \rho\pi$, $B \to \rho K$, $q\bar{q}$, $B\overline{B}$, and rare B in the signal region are 328.7, 11.2, 833.0, 23.3, and 18.8, respectively. We remove the requirements on $M_{\pi^\pm\pi^0}$ and $\cos\theta^\rho_{\rm hel}$ and examine these distributions to verify that the signals reconstructed as $B \to \pi^+\pi^-\pi^0$ are from the two-body decay $B \to \rho\pi$. Figure 2 shows the signal yields in bins of $M_{\pi^\pm\pi^0}$ and $\cos\theta^\rho_{\rm hel}$ for data.

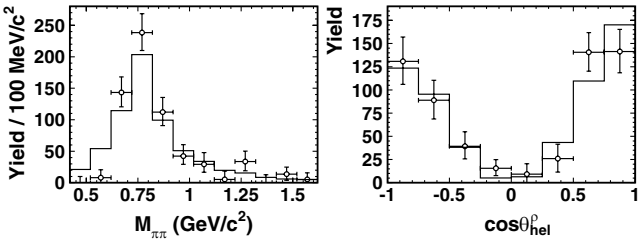

FIG. 2. Signal yields as functions of (left) $M_{\pi\pi}$ and (right) $\cos\theta^\rho_{\rm hel}$ in data. The histograms show the results of $B \to \rho^\pm\pi^\mp$ MC simulation with areas normalized to the total signal yield.

The CP violation parameters are obtained from an unbinned maximum-likelihood fit to the observed proper-time distribution for the $B \to \rho\pi$ candidates in the ($M_{\rm bc}$,ΔE) signal region. The likelihood function describing the proper-time distribution is

$$\mathcal{L} = \prod_{i=1}^{N} \{ f_{\rho\pi} P_{\rho\pi}(\Delta t_i) + f^{\rm wc}_{\rho\pi} P^{\rm wc}_{\rho\pi}(\Delta t_i) + f_{\rho K} P_{\rho K}(\Delta t_i) + f_{q\bar{q}} P_{q\bar{q}}(\Delta t_i) + f_{B\overline{B}} P_{B\overline{B}}(\Delta t_i) + f_{\text{rare } B} P_{\text{rare } B}(\Delta t_i) \}, \quad (4)$$

where the weighting functions f_m ($m = \rho\pi$, ρK, $q\bar{q}$, $B\overline{B}$, and rare B) are determined on an event-by-event basis as functions of $M_{\rm bc}$ and ΔE for each flavor tagging r interval and π^0 momentum range in the laboratory system. The time-dependent probability density functions (Δt PDFs) $P_{\rho\pi}(\Delta t_i)$ for $B \to \rho\pi$ and $P_{\rho K}(\Delta t_i)$ for $B \to \rho K$ are obtained from the true PDFs convolved with the Δt resolution function used in the $\sin 2\phi_1$ measurement [8]. The true PDF for $B \to \rho\pi$ is given by Eq. (1) modified to incorporate the effect of incorrect flavor tagging. The PDF for $B \to \rho\pi$ signal reconstructed with incorrect charge, $P^{\rm wc}_{\rho^\pm\pi^\mp}(\Delta t_i)$, is given by $P_{\rho^\mp\pi^\pm}(\Delta t_i)$. For $B \to \rho K$, $C = S = \Delta S = 0$, $\Delta C = -1$, and $\mathcal{A}^{\rho K} = 0$ is assumed. The resolution function consists of the detector resolution, the shift in vertex position due to secondary tracks originating from charmed particle decays, and smearing due to the approximation $\Delta t \simeq (z_{\rho^\pm\pi^\mp} - z_{\rm tag})/\beta\gamma c$. The Δt PDFs for other backgrounds are all parametrized as $\mathcal{P}_j = (1 - f_j)\delta(\Delta t - \mu^j_\delta) + f_j \exp(-\frac{|\Delta t - \mu^j_\tau|}{\tau_j})$ convolved with R_j ($j = q\bar{q}$, $B\overline{B}$, and rare B), where f_j is the fraction of the background with effective lifetime τ_j. The resolutionlike function R_j for background is given by two Gaussians. The parameters of the Δt PDF for $q\bar{q}$ background are obtained from a fit to sideband data ($5.2\ {\rm GeV}/c^2 < M_{\rm bc} < 5.26\ {\rm GeV}/c^2$ and $\Delta E > -0.15$ GeV). The parameters of the Δt PDFs for $B\overline{B}$ and rare B are obtained from a fit to MC simulations.

The maximum-likelihood fit to the 1215 $\rho\pi$ candidates gives $C_{\rho\pi} = 0.25 \pm 0.17^{+0.02}_{-0.06}$, $\Delta C_{\rho\pi} = 0.38 \pm 0.18^{+0.02}_{-0.04}$, $S_{\rho\pi} = -0.28 \pm 0.23^{+0.10}_{-0.08}$, and $\Delta S_{\rho\pi} = -0.30 \pm 0.24 \pm 0.09$, where the first (second) errors are statistical (systematic). The correlation between $C_{\rho\pi}$ and $\Delta C_{\rho\pi}$ is 0.271 and that between $S_{\rho\pi}$ and $\Delta S_{\rho\pi}$ is 0.284, while correlations between other variables are smaller. The data and fit result are shown in Fig. 3.

The systematic error in $A^{\rho\pi}_{CP}$ includes a possible background asymmetry (± 0.010) and charge asymmetry in the tracking (± 0.012). The charge dependence of tracking efficiency is studied using $D^0 \to K^-\pi^+$ decays from inclusive $D^{*+} \to D^0\pi^+$ and selecting the momentum region corresponding to $B^0 \to \rho^\pm\pi^\mp$ decays. The systematic errors for time-dependent measurements include the uncertainties in the vertex reconstruction, background fraction,

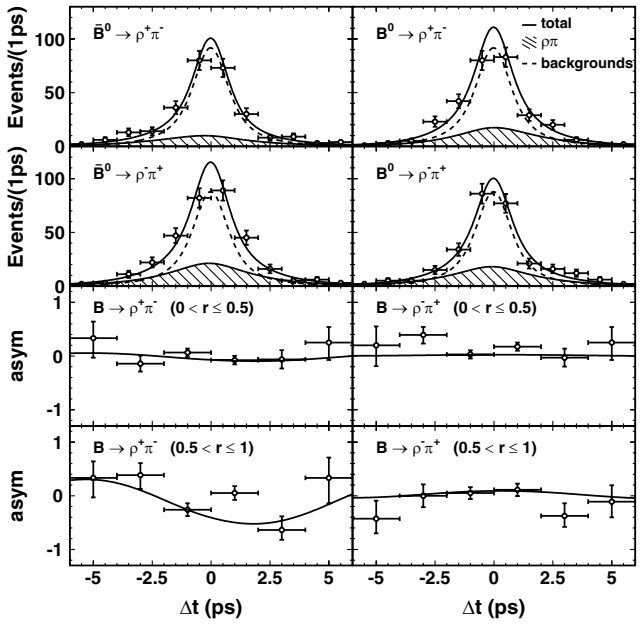

FIG. 3. Δt distributions for $B^0 \to \rho^\pm\pi^\mp$. (Top) B^0 and $\overline{B}^0$ tagged $\rho^+\pi^-$ and $\rho^-\pi^+$ candidates. (Bottom) Raw CP asymmetries in high and low r intervals for $\rho^+\pi^-$ and $\rho^-\pi^+$. The solid curves show the fit results.

background Δt PDF, wrong-tag fractions, $\rho\pi$ and ρK Δt resolution functions, physics parameters (τ_B, Δm_d [12], $\mathcal{A}^{\rho K}$ [13]), and fitting bias. The fitting bias is estimated from MC pseudoexperiments. All other systematic uncertainties are obtained by varying parameters within their errors and repeating the fit. The dominant source of systematic error is the vertex reconstruction ($^{+0.012}_{-0.055}$ for $C_{\rho\pi}$, $^{+0.011}_{-0.038}$ for $\Delta C_{\rho\pi}$, $^{+0.094}_{-0.073}$ for $S_{\rho\pi}$, and $^{+0.089}_{-0.092}$ for $\Delta S_{\rho\pi}$).

We perform various consistency checks. We examine the stability of the results as the $\mathcal{R}$ selection criterion is varied and the asymmetry of the Δt distributions for events in the sideband region. No significant variation or asymmetry is observed. We measure the B^0 lifetime with the $B^0 \to \rho^\pm\pi^\mp$ candidates and find $\tau_{B^0} = 1.56^{+0.13}_{-0.12}$ ps, which is consistent with the world average value [12].

The extraction of ϕ_2 from measurements of time-dependent CP violation parameters in $B \to \rho^\pm\pi^\mp$ decays has been studied in several theoretical approaches [4,14,15]. A Grossman-Quinn type bound [16] based on isospin [SU(2) symmetry] does not significantly limit the penguin diagram contribution due to the large branching fraction for $B^0 \to \rho^0\pi^0$ [17]. Since the number of measurable quantities [six including $\mathcal{B}(B^0 \to \rho^+\pi^-)$] are not sufficient to completely describe the amplitudes for $B^0 \to \rho^\pm\pi^\mp$ decay (8 free parameters), either specific models or additional assumptions are involved, such as QCD factorization [14] or SU(3) flavor symmetry [4]. A recent approach using broken flavor SU(3) implies $\phi_2 = (102 \pm 13 \pm 15)^\circ$ using our results [15]. The first error is experimental, while the second is the uncertainty due to SU(3) breaking effects. Since there are two possible ϕ_2 solutions that correspond to a $\sin(2\phi_2)$ measurement, this result is based on choosing the ϕ_2 solution that is consistent with the established ϕ_1 measurement [8,18].

In summary, using 152×10^6 $B\overline{B}$ pairs, we have measured CP violation parameters for $B^0 \to \rho^\pm\pi^\mp$ decays. We obtain $\mathcal{A}_{CP}^{\rho\pi} = -0.16 \pm 0.10 \pm 0.02$, $C_{\rho\pi} = 0.25 \pm 0.17^{+0.02}_{-0.06}$, $\Delta C_{\rho\pi} = 0.38 \pm 0.18^{+0.02}_{-0.04}$, $S_{\rho\pi} = -0.28 \pm 0.23^{+0.10}_{-0.08}$, and $\Delta S_{\rho\pi} = -0.30 \pm 0.24 \pm 0.09$. These give the direct CP violation parameters $\mathcal{A}_{\rho\pi}^{+-} = -0.02 \pm 0.16^{+0.05}_{-0.02}$ and $\mathcal{A}_{\rho\pi}^{-+} = -0.53 \pm 0.29^{+0.09}_{-0.04}$. These results are consistent with a previous measurement [13]. We find no significant mixing-induced or direct CP violation in $B^0 \to \rho^\pm\pi^\mp$.

We thank the KEKB group for the excellent operation of the accelerator, the KEK cryogenics group for the efficient operation of the solenoid, and the KEK computer group and the NII for valuable computing and Super-SINET network support. We acknowledge support from MEXT and JSPS (Japan); ARC and DEST (Australia); NSFC (Contract No. 10175071, China); DST (India); the BK21 program of MOEHRD and the CHEP SRC program of KOSEF (Korea); KBN (Contract No. 2P03B 01324, Poland); MIST (Russia); MESS (Slovenia); SNSF (Switzerland); NSC and MOE (Taiwan); and DOE (USA).

*On leave from Fermi National Accelerator Laboratory, Batavia, IL 60510.
†On leave from Nova Gorica Polytechnic, Nova Gorica.

[1] M. Kobayashi and T. Maskawa, Prog. Theor. Phys. **49**, 652 (1973).
[2] Belle Collaboration, K. Abe *et al.*, Phys. Rev. D **68**, 012001 (2003).
[3] *BABAR* Collaboration, B. Aubert *et al.*, Phys. Rev. Lett. **89**, 281802 (2002).
[4] For a thorough description of the formalism, see J. Charles *et al.*, hep-ph/0406184.
[5] S. Kurokawa and E. Kikutani, Nucl. Instrum. Methods Phys. Res., Sect. A **499**, 1 (2003).
[6] Belle Collaboration, A. Abashian *et al.*, Nucl. Instrum. Methods Phys. Res., Sect. A **479**, 117 (2002).
[7] G. Fox and S. Wolfram, Phys. Rev. Lett. **41**, 1581 (1978).
[8] Belle Collaboration, K. Abe *et al.*, hep-ex/0408111.
[9] H. Kakuno *et al.*, Nucl. Instrum. Methods Phys. Res., Sect. A **533**, 516 (2004).
[10] ARGUS Collaboration, H. Albrecht *et al.*, Phys. Lett. B **241**, 278 (1990).
[11] Heavy Flavor Averaging Group, http://www.slac.stanford.edu/xorg/hfag/.
[12] K. Hagiwara *et al.*, Phys. Rev. D **67**, 010001 (2002) and 2003 off-year partial update for the 2004 edition available on the PDG WWW pages (http://pdg.lbl.gov/).
[13] *BABAR* Collaboration, B. Aubert *et al.*, Phys. Rev. Lett. **91**, 201802 (2003).
[14] G. Kramer *et al.*, Z. Phys. C **66**, 429 (1995); N. G. Deshpande *et al.*, Phys. Lett. B **473**, 141 (2000); A. Ali

et al., Phys. Rev. D **59**, 014005 (1999); M. Beneke and M. Neubert, Nucl. Phys. **B675**, 333 (2003).
[15] M. Gronau and J. Zupan, Phys. Rev. D **70**, 074031 (2004).
[16] M. Gronau and D. London, Phys. Rev. Lett. **65**, 3381 (1990); Y. Grossman and H. Quinn, Phys. Rev. D **58**, 017504 (1998).
[17] Belle Collaboration, J. Dragic *et al.*, Phys. Rev. Lett. **93**, 131802 (2004).
[18] *BABAR* Collaboration, B. Aubert *et al.*, Phys. Rev. Lett. **87**, 091801 (2001); Phys. Rev. D **66**, 032003 (2002); Phys. Rev. Lett. **89**, 201802 (2002)